Journal of Naval Sciences and Engineering
2025, Vol. 21, No. 1, pp. 25-49 *DOI: 10.56850/jnse.1573476*
Naval Architecture and Marine Engineering/Gemi İnşaatı ve Gemi Makineleri Mühendisliği

RESEARCH ARTICLE

**An ethical committee approval and/or legal/special permission has not been required within the scope of this study.*

NUMERICAL INVESTIGATION OF THE SELF PROPULSION PERFORMANCE OF KCS HULL

Muhammed ÇINAR[1*]
Ferhat DİKMEN[2]
Hakan UÇAR[3]

[1]*Yıldız Technical University, Department of Mechanical Engineering, Istanbul, Turkey, muhammed.cinar@std.yildiz.edu.tr*

[2]*Yıldız Technical University, Department of Mechanical Engineering, Istanbul, Turkey, dikmen@yildiz.edu.tr*

[3]*Turkish Naval Forces, Design Project Office, Istanbul, Turkey, hucar@pirireis.edu.tr*

Received: 28.10.2024 **Accepted: 03.01.2025**

ABSTRACT

This paper presents a numerical investigation for KCS (Kriso Container Ship) hull self-propulsion performance characteristics by using RANS (Reynolds-Averaged Navier-Stokes) solution method and k-ω SST (Shear Stress Transport) turbulence modeling. Before examining the hull-propeller interaction, the propeller open water validation study is carried out. To estimate the propulsive performance of the KCS hull, thrust coefficient (K_T) and torque coefficient (K_Q) are calculated and local velocity wake fields around the propeller and pressure distribution on the hull are simulated. In order to solve the viscous flow around the propeller and hull more accurately, the optimum mesh element size is determined by performing a mesh sensitivity analysis. In order to validate the numerical method used in the current study, the calculated values are compared with the test results. As a results of these comparisons, it is clearly proved that results obtained from CFD (Computational Fluid Dynamics) make a good agreement with the experimental results. These numerical results indicate that the significant influence of the mesh sensitivity analysis on the calculated open water and self-propulsion performance characteristics and CFD prediction of propeller/hull interaction is much more cost effective and time saving compared to the towing tank tests.

Keywords: *Mesh Sensitivity, Open Water, Propeller-Hull Interaction, Self Propulsion, Validation.*

MAKALENİN TÜRKÇE BAŞLIĞI

ÖZ

Bu çalışma, RANS çözüm yöntemi ve k-ω SST türbülans modellemesi kullanarak KCS teknesi sevk performansının sayısal bir inceleme sunmaktadır. Gövde-pervane etkileşimini incelemeden önce, pervane açık su doğrulama çalışması yapılmıştır. KCS teknesinin sevk performansını tahmin etmek için itme katsayısı (K_T) ve tork katsayısı (K_Q) hesaplanarak pervane etrafındaki hız dağılımı ile gövde üzerindeki basınç dağılımı simüle edilmiştir. Pervane ve tekne etrafındaki viskoz akışı daha doğru bir şekilde çözmek için, bir ağ hassasiyet analizi yapılarak optimum ağ eleman boyutu belirlenmiştir. Mevcut çalışmada kullanılan sayısal yöntemin doğruluğunu ortaya koymak için hesaplanan değerler test sonuçlarıyla kıyaslanmıştır. Bu kıyaslamalar sonucunda, nümerik analiz ile elde edilen sonuçların test sonuçları ile iyi bir uyum gösterdiği açıkça kanıtlanmıştır. Bu sayısal sonuçlar, ağ hassasiyet analizinin açık su ve sevk performansı üzerindeki önemli etkisini ortaya koymakla birlikte pervane/tekne etkileşiminde hesaplamalı akışkanlar dinamiği kullanılmasının, çekme tankı testlerine kıyasla çok daha maliyet etkin olduğunu ve zaman tasarrufu sağladığını göstermiştir.

Anahtar Kelimeler: *Ağ Duyarlılığı, Açık Su, Pervane-Gövde Etkileşimi, Sevk Performansı, Doğrulama.*

1. INTRODUCTION

Computational Fluid Dynamics (CFD) is a burgeoning field that is swiftly gaining recognition in various sectors, including shipbuilding and offshore industries, primarily due to advancements in computational technology. As the capabilities of hardware continue to enhance, researchers and engineers can undertake more sophisticated simulations with improved accuracy, resulting in more reliable predictions of fluid behavior across different settings. Additionally, the capacity to model realistic scenarios without the necessity for extensive physical prototypes not only streamlines the design process but also leads to significant cost reductions. As industries increasingly focus on efficiency and sustainability, the utilization of CFD is expected to expand further, solidifying its role as a vital resource in both engineering and scientific exploration. In shipbuilding industry, determination of the hull self-propulsion performance is one of the compulsory steps considered when

assessing hull hydrodynamic performance in the early stage of ship design. The self-propulsion parameters that are necessary for ship performance prediction can be obtained by relying on computational methods or performing model tests. Scale model testing is a universally applicable approach to investigate hull self-propulsion performance. However, the high development of advanced numerical methods of the ship and propeller design process provide that towing tank tests were replaced by the advanced numerical methods as computational and time cost were decreased. In the early stage of hull design, the open water towing tank tests were usually preferred to identify the open water characteristics of the propeller and investigate the propeller-hull interaction. Thus, CFD methods are now becoming more prevalent way for solving challenging hull and propeller optimization problems where modifications in hull and propeller geometries are required. Various hydrodynamic problems have been analyzed using the KCS (KRISO Container Ship) vessel. One of the most important studies conducted is the analysis of hull self-propulsion performance. Carrica et al. developed a numerical approach to predict the self-propulsion point for three benchmark ship designs. Their methodology aimed to achieve a balance between thrust and resistance by manipulating the rotational speed of the propeller, using computational fluid dynamics (CFD) for their analysis. Shen et al. examined the self-propulsion capabilities and maneuvering behavior of the KRISO Container Ship (KCS) through simulations conducted with the open-source CFD software OpenFOAM, utilizing a dynamic overset grid technique to facilitate their study. In their research, Castro et al. performed full-scale self-propulsion calculations for the KCS hull, finding that the propeller demonstrated improved efficiency at full scale compared to the results obtained from model scale simulations. Zhang et al. employed two methods to calculate the flow around KCS hull with a propeller. The first method is the body force approach, which is straightforward and quick. However, this method may not clearly capture the primary features of the propeller's effects. The second method is the sliding mesh technique, known for its accuracy but also for being computationally intensive. The results indicate that both approaches are viable for studying the interaction between the hull and the propeller. Wan et al.

investigated ship self-propulsion performance in different shallow water conditions. They conducted numerical simulations using their own proprietary solver, naoe-FOAM-SJTU, which is built on the open-source platform OpenFOAM. This solver primarily features a dynamic overset grid module. They utilized proportional-integral (PI) controller to regulate the propeller's rotational speed in order to attain the target ship speed. Their current method is suitable for predicting self-propulsion in shallow water conditions. Feng et al. examined the effect of water depth on ship resistance, selecting several significant limited water depths to perform towed resistance simulations for a KRISO container ship (KCS). The study calculated the resistance and attitude for both the scaled model and the full-scale KCS across various water depths. Carrica et al. described two simulations of the KCS model with motion. The initial scenario explores self-propulsion at the model scale, enabling free sinking and trimming, and utilizes the rotating discretized propeller. The second scenario addresses pitch and heave in regular head waves. The computations were performed using CFD Ship-Iowa version 4.5, a RANS/DES CFD code tailored for ship hydrodynamics.

In order for computational fluid dynamics to provide the most accurate and closest results to the experimental data, it is crucial to define the problem in detail and to develop a physical and mathematical model that is appropriate for the specific problem being investigated. In addition to these, applying the most suitable mesh structure to the created numerical model is a very important factor that affects the numerical result obtained. The element size of mesh applied in numerical analyzes during mesh generation process cause the investigated variable to change quantitatively. Consequently, this study conducts a mesh sensitivity analysis following the recommended procedure (ITTC, 2017). This analysis aims to determine the optimal mesh element size that yields more realistic computational results, as the number of mesh elements significantly influences the torque and thrust values. Additionally, this approach helps to minimize excessively long solution times and reduce the demand for high computational requirements. The self-propulsion validation was carried out by comparing the self-propulsion performance

characteristics wake fraction (w), thrust coefficient (K_T), and torque coefficient (K_Q) obtained from present CFD and measured with the experiment.

2. NUMERICAL THEORY

The Reynolds Averaged Navier-Stokes (RANS) solver equations are employed in the present study. When the Reynolds averaging approach for turbulence modeling is applied, the governing equations (Navier–Stokes equations) are written for the mass and momentum conservation in cartesian tensor form;

$$\frac{\partial \rho}{\partial t} + \frac{\partial u_i}{\partial x_i} = 0 \tag{1}$$

$$\frac{\partial}{\partial t}(\rho u_i) + \frac{\partial}{\partial x_j}(\rho u_i u_j) = -\frac{\partial p}{\partial x_i} + \frac{\partial}{\partial x_j}\left[\mu\left(\frac{\partial u_i}{\partial x_j} + \frac{\partial u_j}{\partial x_i} - \frac{2}{3}\delta_{ij}\frac{\partial u_i}{\partial x_i}\right)\right] + \frac{\partial}{\partial x_j}\left(-\rho\overline{u_i'}\,\overline{u_j'}\right) \tag{2}$$

where x_i is cartesian coordinates, u_i is the corresponding velocity components, p is the pressure, ρ is the density, δ_{ij} is the Kronecker delta and μ is the kinematic viscosity. Also, $-\rho\overline{u'_i u'_j}$ is the Reynold stress term which has been closed by using the k–ω SST (Shear Stress Transport) turbulence model because of its high accuracy and reliability to resolve the adverse pressure gradient flows and flow around the propeller. This model ensures that both the near-wall and far-field zones are appropriately solved because an additional cross-diffusion term ($CD_{k\omega}$) is included. The transport equations used for solving the transport variables k and ω are as follows:

For turbulent kinetic energy k,

$$\frac{\partial k}{\partial t} + U_j\frac{\partial k}{\partial x_j} = P_K - \beta^* k\omega + \frac{\partial}{\partial x_j}\left[(\nu + \sigma_k \nu_T)\frac{\partial k}{\partial x_j}\right] \tag{3}$$

For turbulence dissipation rate;

$$\frac{\partial \omega}{\partial t} + U_j\frac{\partial \omega}{\partial x_j} = aS^2 - \beta\omega^2 + \frac{\partial}{\partial x_j}\left[(\nu + \sigma_\omega \nu_T)\frac{\partial \omega}{\partial x_j}\right] + 2(1-F_1)\sigma_{\omega^2}\frac{1}{\omega}\frac{\partial k}{\partial x_i}\frac{\partial \omega}{\partial x_i} \tag{4}$$

Closure coefficients and auxilary relations;

$$F_1 = \arctan\left\{\left\{\min\left[\max\left(\frac{\sqrt{k}}{\beta^* \omega y}, \frac{500\nu}{y^2 \omega}\right), \frac{4\sigma_{\omega^2} k}{CD_{k\omega} y^2}\right]\right\}^4\right\} \tag{5}$$

Kinematic Eddy Viscosity;

$$\nu_T = \frac{a_1 k}{\max(a_1 \omega, SF_2)} \tag{6}$$

$$F_2 = \tanh\left[\left[\max\left(\frac{2\sqrt{k}}{\beta^* \omega y}, \frac{500\nu}{y^2 \omega}\right)\right]^2\right] \tag{7}$$

$$P_k = \min\left(\tau_{ij} \frac{\partial U_i}{\partial x_j}, 10\beta^* k\omega\right) \tag{8}$$

where $CD_{k\omega}$ is the cross-diffusion term;

$$CD_{k\omega} = \max\left(2\rho\sigma_{\omega^2} \frac{1}{\omega} \frac{\partial k}{\partial x_i} \frac{\partial \omega}{\partial x_i}, 10^{-10}\right) \tag{9}$$

The convergence criterion of 10^{-6} was used for this analysis.

2.1. Basic Characteristics

The propeller self-propulsion verification analysis is performed by comparing certain dimensionless coefficients of the propeller obtained from computational analysis. Before the propeller-hull interaction analysis, it has to be validated the propeller open water characteristics.

The dimensionless performance coefficients specifying the general performance characteristics of the propeller are thrust coefficient (K_T), torque coefficient (K_Q) and

advance coefficient (J) values. These dimensionless coefficients are calculated as follows depending on the inputs of propeller thrust (T), propeller torque (Q), fluid density (ρ), rate of revolutions of the model propeller (n), propeller diameter (D) and speed of advance of the model propeller (V). Based on these coefficients, the propeller open water efficiency (μ_0), the fluid velocity at suction side of the propeller (V_a), nominal wake fraction (ω_n), effective wake fraction(ω_t) is obtained (Carlton, 2006; ITTC, 2014).

$$K_T = \frac{T}{\rho n^2 D^4} \tag{10}$$

$$K_Q = \frac{Q}{\rho n^2 D^5} \tag{11}$$

$$J = \frac{Va}{nD} \tag{12}$$

$$\mu_0 = \frac{K_T}{K_Q}\frac{J}{2\pi} \tag{13}$$

$$\omega = \frac{Vs - Va}{Vs} \tag{14}$$

3. METHODOLOGY OF OPEN WATER VALIDATION

The open water and self-propulsion experiments were conducted at the Ship Research Institute, now known as the National Maritime Research Institute (NMRI), utilizing a towing tank characterized by dimensions of 400 meters in length, 18 meters in width, and 8 meters in depth. The results of the tests were shared at the International Workshop on Computational Fluid Dynamics in Ship Hydrodynamics, which took place in Gothenburg (Tsukada et al., 2000; Fujisava et al., 2000) and

Tokyo (Kim J., 2015). The open water CFD validation was performed using a 1:31,5994 scale model of the KP505 propeller. The RANS (Reynold Averaged Navier Stokes) governing equations were used for numerical calculation and k-ω SST was used for turbulence modeling.

For the propeller analysis, two solution geometries (control volumes) were created for the flow simulation. The moving control volume is located inside of the external control volume and is defined as rotor. The external control volume is stationary and defined as stator. CFD solver keeps the surfaces in the moving control volume stable and rotates the fluid around the surface. The propeller model to be used in the open water propeller validation analysis was made in the three-dimensional solid model program and an external domain suitable for the model propeller dimensions was created on the outside. In determining the dimensions of the external flow volume, the studies obtained as a result of the literature (Seok et al., 2019; Seo et al., 2010) were taken as an example. In these studies, the KP505 propeller was used for model-scale open water verification analysis and the height of the external flow volume surrounding the propeller was taken as 1,2 times the propeller diameter (D). In this study, the height of the external flow volume was taken as 1,2D, the width of the external flow volume of the propeller was determined as 0,31 times the diameter of the propeller. For the analysis performed using the five-bladed model, the solution volume height was determined as 5 times the propeller diameter, and the solution volume length was determined as 12 times the propeller diameter.

3.1. KP505 Propeller Model Geometry

The KP505 test propeller was designed and manufactured by KRISO (Korea Research Institute of Ships and Ocean Engineering) with a model scale ratio of 1:31,5994 and sent to the Ship Research Institute (SRI) to be used in open water tests. The propeller (SRI MP No.460) basic parameters and the model geometry of the KP505 propeller are given in Table 1 and Figure 1 respectively.

Table 1. *Principal particulars of tested propeller (Tsukada et al., 2000).*

Characteristics	Value
Ship Model Name	KP505
Diameter(m)	0,2500
Boss Ratio	0,1800
Pitch Ratio @ 0,7R	0,9967
Ratio of Expanded Blade Area	0,800
Angle of Skew (degree)	32,0
Blade Number	5
Rotation Direction	Right
Section of Blade	NACA66 Thickness

The model geometry is officially provided by Tokyo 2015 CFD Workshop.

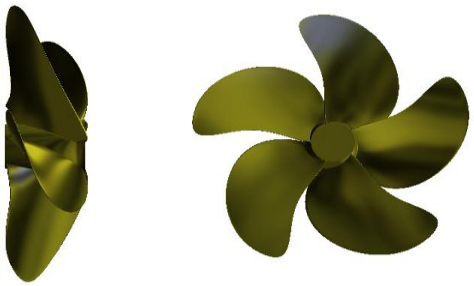

Figure 1. *KP505 propeller model.*

3.2. Mesh Dependency Study

In the mesh process mesh sensitivity analysis was performed to determine the optimum mesh size as shown in Table 2. Changes between medium-fine $\varepsilon_{21}=S_2-S_1$ and coarse-medium $\varepsilon_{32}=S_3-S_2$ solutions are used to define the convergence ratio $R=\varepsilon_{21}/\varepsilon_{32}$ where S_1, S_2, S_3 correspond to solutions with fine, medium, and coarse input parameter, respectively, corrected for iterative errors. The analysis was repeated by reducing the mesh size by $\sqrt{2}$ times the previous one (ITTC, 2017).

Three convergence conditions are possible:

(i) Monotonic convergence: $0 < R < 1$

(ii) Oscillatory convergence: $R < 0$

(iii) Divergence: $R > 1$

Table 2. *Mesh sensitivity analysis results.*

	Blade Mesh Size (mm)	S	Thrust (N)	Torque (Nm)	Thrust		Torque		R_{thrust}	R_{torque}
					ε_{21}	ε_{32}	ε_{21}	ε_{32}		
Study -1	2,83	S_3	153,17	6,43	-0,47	-0,44	0,057	0,068	1,07	0,83
	2,00	S_2	153,61	6,37						
	1,41	S_1	154,08	6,31						
Study -2	2,00	S_3	153,61	6,37	-0,45	-0,47	0,072	0,057	0,96	1,27
	1,41	S_2	154,08	6,31						
	1	S_1	154,53	6,24						
Study -3	1,41	S_3	154,08	6,31	0,63	-0,45	0,053	0,072	-1,4	0,74
	1	S_2	154,53	6,24						
	0,71	S_1	153,90	6,19						
Study -4	1	S_3	154,53	6,24	0,39	0,63	0,033	0,053	0,62	0,63
	0,71	S_2	153,90	6,19						
	0,5	S_1	153,51	6,15						

In study 4, since the condition $0<R<1$(R_{thrust} =0,62 and R_{torque} =0,63) was satisfied for both parameters, convergence was achieved and the optimum mesh size was determined. The change of thrust and torque according to the number of elements is given in Figure 2. Sensitivity analysis for propeller thrust and torque values was performed under the condition of propeller advanced coefficient J = 0,5.

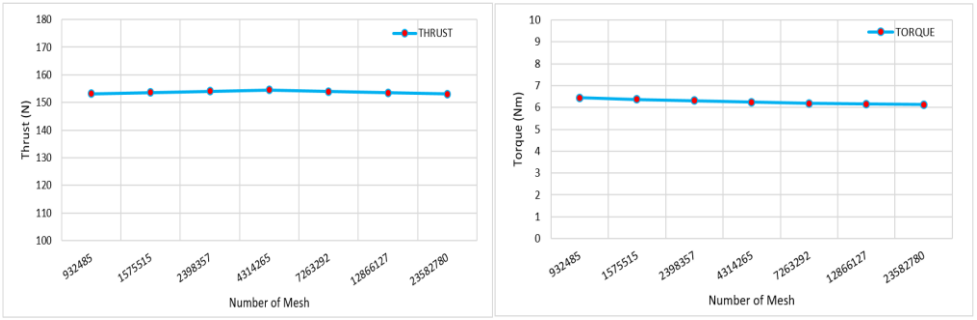

Figure 2. a) *Change of thrust according to the number of elements,* ***b)*** *Change of torque according to the number of elements.*

3.3. Grid Structure and Boundary Conditions of Propeller

As a result of the mesh sensitivity analysis 0,5 mm tetrahedral mesh on the blade and 2 mm tetrahedral mesh on the hub were employed. Quality criterias that determine the mesh element quality during the process of creating the mesh structure were selected as the $y+$ value, skewness and orthogonal quality. In order to model the fluid motion around the propeller accurately, a boundary layer structure was created on the propeller blade. The mean boundary layer was divided into 12 layers. The total boundary layer thickness was determined by increasing 1,2 times from the inside out for each layer. The mesh structure of the propeller blades is shown in Figure 3.

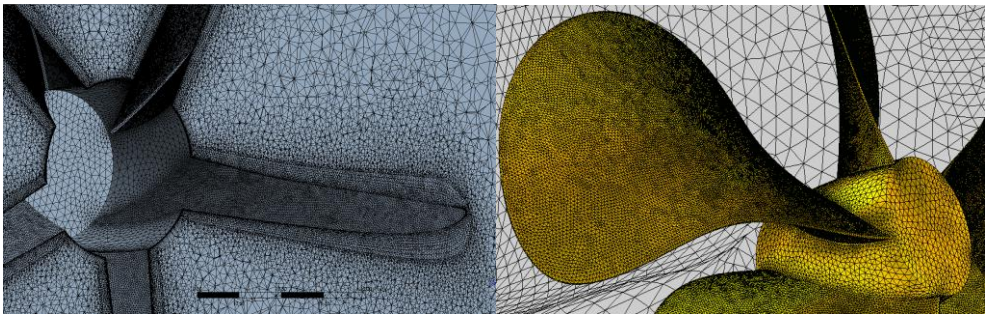

Figure 3. *Mesh structures of boundry layer, hub and blade.*

In the open water CFD analyzes the k-ω SST method was employed for the turbulence model. Second order and high-resolution methods were used in turbulence model and solver algorithms. Analyzes were performed with transient condition.

The cylindrical computational domain of the propeller and the boundary conditions around it are given in Figure 4. No-slip wall condition was applied on the propeller and its hub. On the other hand, free-sleep wall condition for the cylindrical boundary around the propeller was applied. Outlet pressure was set to zero on the exit boundary.

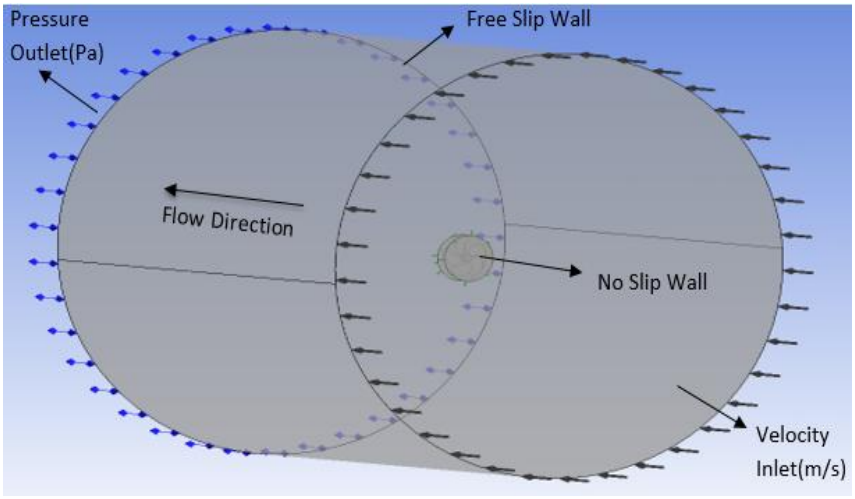

Figure 4. *Boundary conditions of propeller.*

In order to obtain the KP505 propeller open water performance as a result of the CFD analysis, the computational simulation is carried out by means of varying the inlet velocity with a constant angular velocity of n=12 rps (rate per second) for all advance ratios. V_A is the value to be entered as propeller inlet velocity. The velocity values required to be entered in each advance coefficient were obtained by using Eq. (12) as given in Table 3.

Table 3. *Inlet velocities depending on advance coefficients.*

J	**V_A(m/s)**
0,1	0,3
0,2	0,6
0,3	0,9
0,4	1,2
0,5	1,5
0,6	1,8
0,7	2,1
0,8	2,4

3.4. Open Water CFD Results and Evaluations

The comparison of the results obtained from CFD and test are given in Table 4.

Table 4. *Comparing of CFD and test results (Tsukada et al., 2000).*

		Thrust Coefficient (K_T)			Torque Coefficient (K_Q)			Efficiency(η)		
Open Water J	V_{inlet}	CFD K_T	Open Water K_T	Error [%]	CFD $10*K_Q$	Open Water $10*K_Q$	Error [%]	CFD	Open Water	Error [%]
0,1	0,3	0,463	0,482	-3,88	0,674	0,678	-0,50	0,109	0,113	3,12
0,2	0,6	0,422	0,435	-3,02	0,621	0,622	-0,17	0,216	0,223	3,03
0,3	0,9	0,375	0,387	-3,22	0,562	0,557	0,97	0,318	0,332	4,22
0,4	1,2	0,324	0,336	-3,48	0,501	0,497	0,75	0,412	0,431	4,33
0,5	1,5	0,272	0,285	-4,44	0,437	0,437	0,02	0,496	0,519	6,99
0,6	1,8	0,219	0,235	-6,52	0,372	0,376	-1,00	0,564	0,597	5,60
0,7	2,1	0,167	0,185	-9,91	0,306	0,311	-1,71	0,608	0,665	8,66
0,8	2,4	0,113	0,137	-16,99	0,237	0,247	-4,17	0,612	0,705	13,24

In order to understand the difference between the values measured by experiment (Tsukada et al., 2000) and numerical analysis more clearly, a comparison graph was created with the calculated and measured results as shown in Figure 5.

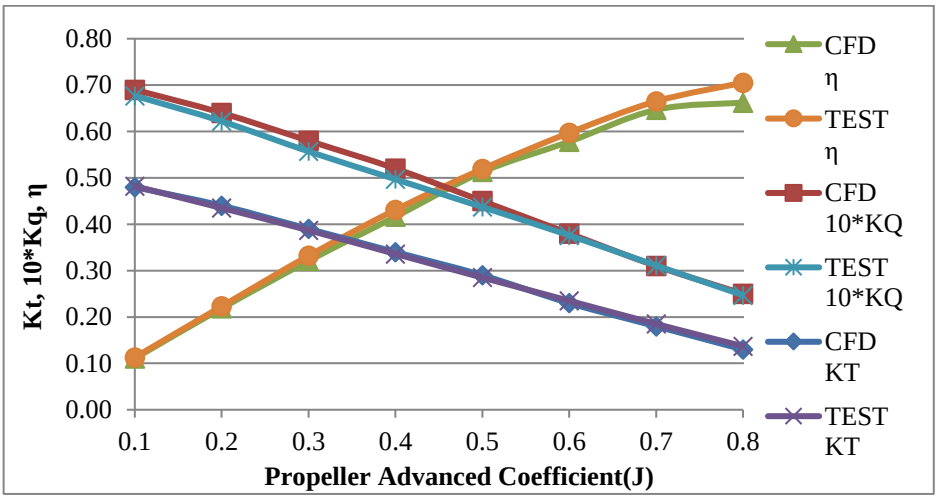

Figure 5. *Comparison of thrust coefficient, torque coefficient, and open water efficiency between the experimental and computational results.*

When examining the open water propeller graph, it is observed that after an advance ratio of J=0.5, the propeller efficiency deviates from the test data, and after a certain advance ratio, the propeller efficiency begins to decrease. Similar to the abrupt loss of force experienced by a rudder blade beyond an angle of 30 degrees, high advance ratios result in an increase in flow velocity acting on the propeller blades. This leads to a diminished influence of shear forces and a subsequent predominance of viscous forces in the NACA airfoil propeller, ultimately resulting in stall conditions on the blades. Beyond a certain advance ratio, the excessively elevated Reynolds number significantly reduces the shear forces generated by the propeller. This phenomenon is evident in the efficiency curves of the open water propeller, as observed in both experimental data and numerical analysis results. However, discrepancies in the stall point of the propeller arise due to variations in the environmental conditions of the test and the inherent error margins associated with the numerical analysis. The KP505 propeller open water performance test results and the results obtained from CFD are examined, an average of 6,43% error rate in thrust and an average of 0,73 % error rate in torque have been achieved. Thus, it was determined that the difference between the computational results and the test results was at a reasonable level. behind the propeller were obtained. The rudder-hull intreraction was ignored. CFD validation was performed using a 1:31,5994 scale model of the KP505 propeller and KCS hull. The k-ω SST method was employed for the turbulence model and second order and High Resolution were used in turbulence modeling and solver algorithms.

4. METHODOLOGY OF SELF PROPULSION VALIDATION

The KCS self-propulsion tests were carried out at the SRI (now NMRI) 400 m towing tank without the rudder. During the towing tank tests, two local velocity measurements were carried out at without and with working propeller model conditions at 0,25D behind the propeller plane. In this study, as in the experiment, examination of the hull-propeller interaction is one of the most important case, so the self-propulsion validation study consists of two different analyses. In the first case, the nominal wake field and nominal velocity coefficient that would occur

0.25D(x/L=0,491) meters behind the propeller plane by performing analysis on without propeller condition was simulated. Afterwards, the effective wake field at 0,25D downstream side of the propeller disc for working propeller condition was simulated. With the second analysis, the effective wake field and effective velocity coefficient behind the propeller were obtained. The rudder-hull interaction was ignored. CFD validation was performed using a 1:31,5994 scale model of the KP505 propeller and KCS hull. The k-ω SST method was employed for the turbulence model and second order and High Resolution were used in turbulence modeling and solver algorithms.

4.1. KCS Hull Model Geometry

The experimental conditions and model geometry of KCS hull was provided by KRISO. The hull was manufactured at the SRI using the lines provided by KRISO with a scale ratio of 1:31,5994. The principal particulars SRI M. S.No. 631 are shown in Table 5.

Table 5. *Principal particulars of tested ship (Tsukada et al., 2000).*

Characteristics	Symbol	Unit	Value
Ship Model Name	-	-	SRI M. S. No. 631
Distance Between Perpendiculars	L_{PP}	m	7,2786
Load Water Line Length	L_{WL}	m	7,3568
Breadth	B	m	1,0190
Depth	D	m	0,5696
Ship Draft	d	m	0,3418
Area of Wetted Surface w/o Rudder	S_W	m^2	9,4984
Area of Rudder Surface	S_B	m^2	0,0741
Displacement of w/o Rudder	∇	m^3	1,6497
Buoyancy Center from Midship (Backward, +)	l_{CB}	$\%L_{PP}$	1,48
Coefficient of Blockage	C_B	-	0,6508
Coefficient of Midship	C_M	-	0,9849
Coefficient of Prismatic	C_P	-	0,6608

The distance between perpendiculars (L_{PP}), the load water line length (L_{WL}) and the draft of the ship model are 7,2786 m, 7,3568 m and 0,3418 m respectively for model scale. Since the bottom of the ship's waterline(draft) will be considered in the propeller propulsion performance validation analysis, the ship model was trimmed from the waterline in the 3D program as shown in Figure 6.

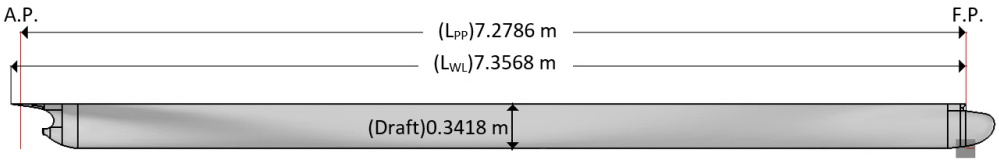

Figure 6. *KCS hull trimmed model.*

4.2. Grid Structure and Boundary Conditions of Hull

In the mesh generation process, 11 million mesh elements were used in the control volume at where 12 mm tetrahedral mesh element in hull form and 6 mm tetrahedral mesh element in propeller were used. In order to keep the y+ value between 30-300, 12 layers of boundary layer with a total thickness of

20 mm were applied to the hull form, and 12 layers boundary layer was added to the propeller geometry with a total thickness of 2,4 mm.

As a result of the mesh generation, the stationary fluid region and the rotating propeller disc contain about 3,43 million and 7,44 million cells, respectively. The mesh structure of the propeller blades is shown in Figure 7.

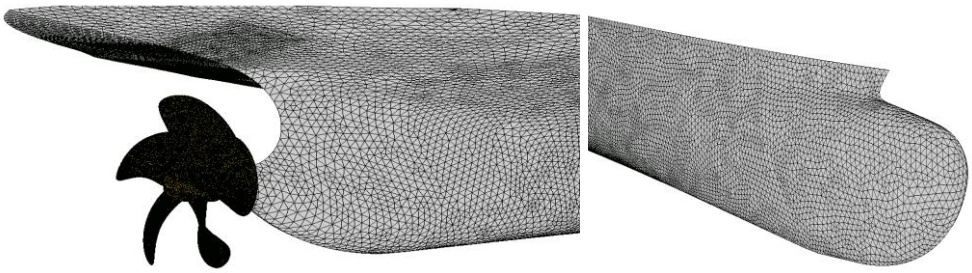

Figure 7. *The mesh structure of hull.*

The ship velocity and propeller rotational velocity was kept at 2,196 m/s and 9,5rps respectively. According to the test report, the Reynolds number (Re) was 1,406×107 at 15,1°C and the water density (ρ) was 999,4428 kg/m^3 in the computational analyzes. The angular velocity of the propeller model was 9,5 rps. The boundary conditions and computational domain are given in Figure 8.

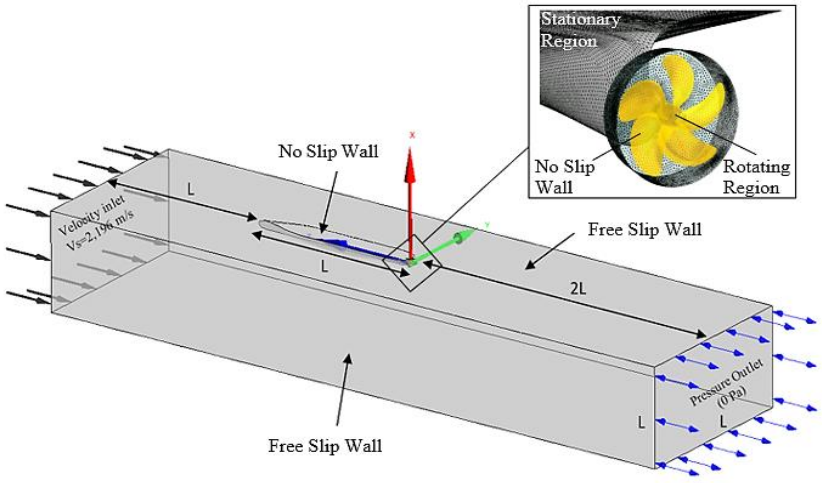

Figure 8. *Computational domain and boundary conditions.*

5. NUMERICAL RESULTS OF HULL SELF PROPULSION

In the without propeller condition, analysis was performed without the propeller attached to the ship stern. As a result of the analysis, the nominal velocity coefficient at a distance of 0,25D from the propeller plane was compared with the test results and the results of other CFD studies with different solvers in the literature as given in Table 6.

Table 6. *Measured (Fujisava et al., 2000) and calculated nominal wake fractions*

	$1-\omega_N$
Fujisava et al. (NMRI Test)	0,686
Present CFD	0,665
Kinaci et al.	0,741
Carrica et al.	0,723
Carrica et al.-RANS	0,740
Carrica et al.-HSVA	0,745
Carrica et al.-SVA	0,721
Carrica et al.-KRISO	0,723
Carrica et al.-OPU	0,634
Shen et al.	0,742

As given in Table 6, an acceptable difference between test result and calculated value for nominal wake fraction was achieved. The error rate between present CFD and the experiment is 3,6 %. The nominal velocity distribution is compared with the test result as given in Figure 9.

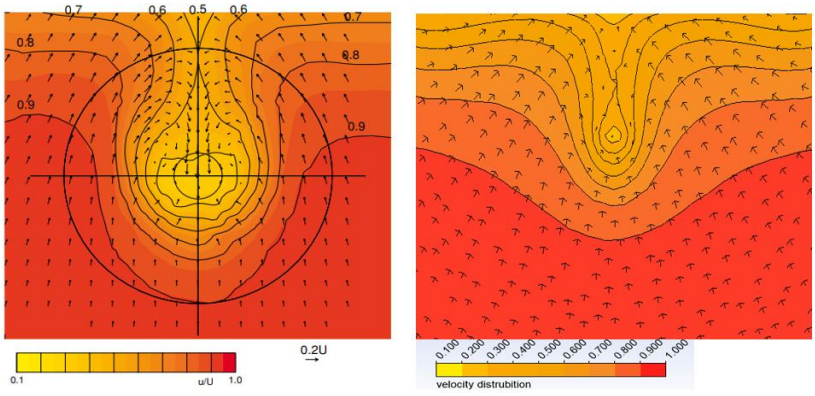

Figure 9. *Nominal wake fields at distance of 0.25D (x/L=0,491) from the propeller plane (left-test (Fujisava et al., 2000), right-HAD)*

When the comparison of the CFD and test results for the without-propeller condition was examined, it was evaluated that a good convergence was obtained to the experimental results.

In the working propeller condition, the KP505 propeller was situated at x/L = 0,4825, meaning it was positioned 0,0175L (or 127,3 mm) in front of the Aft Perpendicular (A.P.) of the hull. For the self-propulsion validation study, the velocity distribution at 0,25*D downstream of the propeller disc, surface pressure distribution on the hull, effective wake fraction ($1-\omega_t$) and self-propulsion performance coefficients (K_T, K_Q) from CFD were compared with those obtained from the experiment.

Due to the propeller-hull interaction, transient condition was employed for the self-propulsion analyzing but first, the convergence of the hull form was achieved in the first 600 iterations with the time-independent "Steady-Frozen Rotor" method in a time step of 0,072 seconds. Then, the time-independent "Steady" analysis was stopped and duplicated. The new created solution group was connected to the analysis that resulted in the time-independent "Steady" and 720 iterations were continued with the time-dependent "Transient Rotor-Stator" solution method to investigate the propeller-hull interaction. At the end of the analysis, the convergence of the propeller thrust and torque coefficients were achieved, and the analysis was completed.

The comparison of the revolutions, thrust coefficient and torque coefficient obtained from present CFD, EFD and other CFD simulations is given in Figure 10.

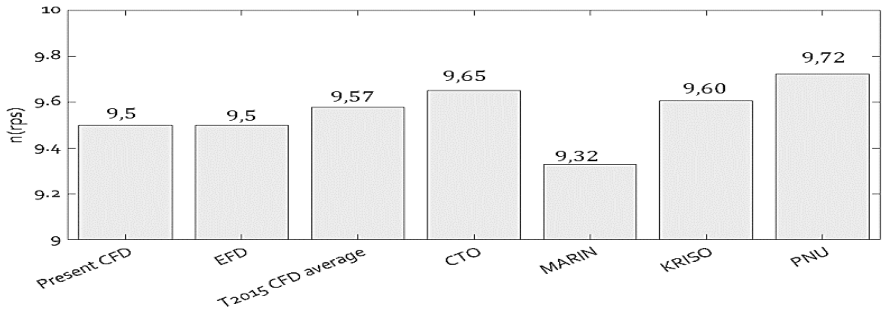

(a)

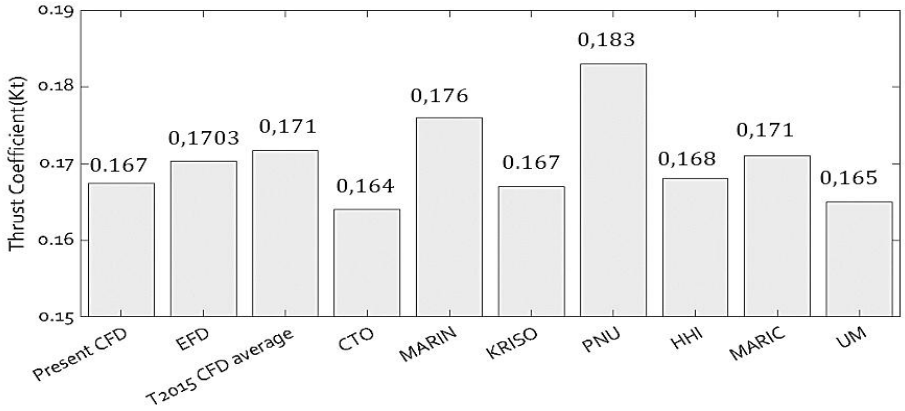

(b)

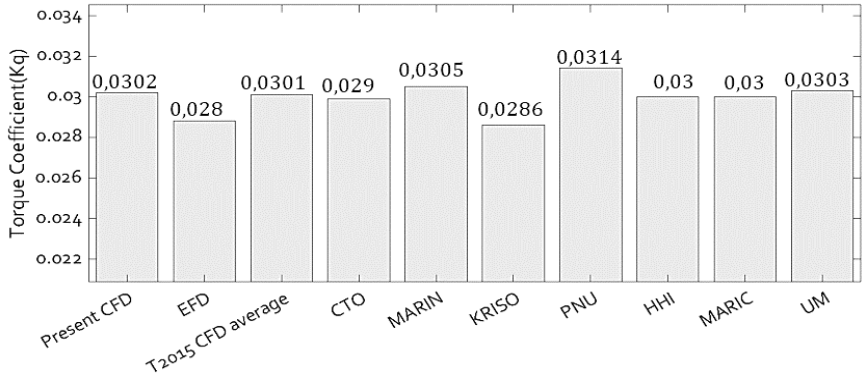

(c)

Figure 10. *The comparison of the rotational speed, thrust and torque coefficient obtained from present CFD, EFD and other CFD simulations (Kim, 2015).*
a) *Rotational speed,* ***b)*** *Thrust coefficient,* ***c)*** *Torque coefficient.*

As shown in Figure 10, the current numerical simulation results show good agreement with the experimental data and the average values of the Tokyo 2015 CFD results. The relative differences between the test result and present CFD for K_T and K_Q are 1,7% and 4,63%, respectively. Furthermore, the effective velocity distribution behind the propeller disc and the pressure distribution on the hull surface created by the propeller-hull interaction were compared with the test. The measured and calculated effective wake distribution at x/Lpp=0,491 was simulated as shown in Figure 11.

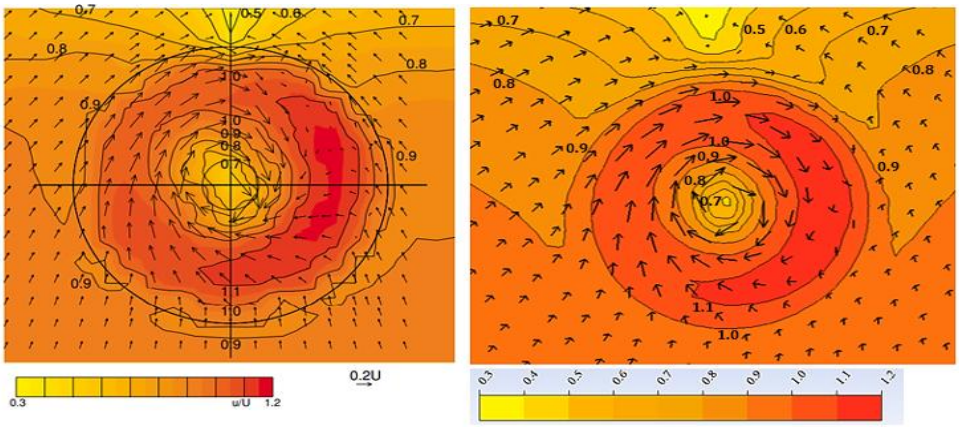

Figure 11. *Local velocity fields for working propeller condition 0,25D downstream of the propeller disc (Left-Test (Fujisava et al., 2000), Right-HAD)*

The measured and calculated pressure distribution on the KCS hull surface is shown in Figure 12.

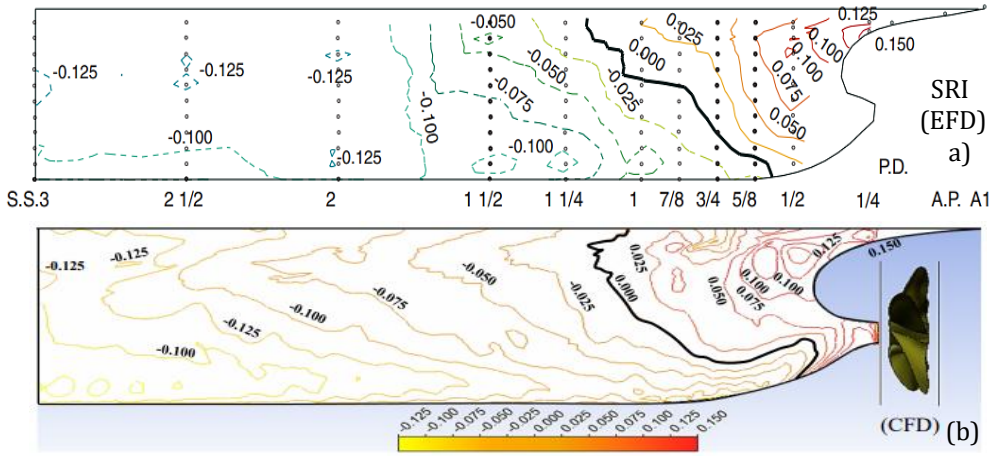

Figure 12. *Surface pressure distribution of KCS hull measured at SRI 400 m Towing Tank (Tsukada et al., 2000). Hull surface pressure distribution (C_p contours) from CFD (Top: Test (Tsukada et al., 2000), Bottom: CFD).*

According to the figures, the results of the flow simulation for working propeller condition, in terms of the effective wake field around the propeller disc and pressure

distribution on hull demonstrate a good agreement with those obtained from the experiment.

Furthermore, the effective wake fraction was also calculated by using Eq. (14) and compared with result obtained from the experiment and other computational results reported at the CFD Workshop Tokyo 2015.

$$\omega_t = \frac{Vs - Va}{Vs}$$

$$\omega_t = \frac{2{,}196 - 1{,}74189}{2{,}196}$$

$$1\text{-}\omega_t = 0{,}793$$

The comparison of effective wake fraction $(1\text{-}\omega_t)$ between test result and other computational results are given in Table 7.

Table 7. *Comparisons between measured (Kinaci et al., 2018) and calculated effective wake fractions*

	n	$1\text{-}\omega_t$
Present CFD	9,5	0,793
NMRI (Exp.)	9,68	0,792
Kinaci et al.	9,5	0,795
Carrica et al.- MOERI	9,38	0,779
Carrica et al.- HSVA	9,56	0,789
Carrica et al.- SVA	9,5	0,765
Carrica et al.- OPU	9,53	0,789

The error rate between present CFD and the experiment is 0,12 %. Thus, a significant convergence to the experimental result is obtained. After the self-propulsion validation analysis was completed, the pressure distribution of the KCS hull area on the propeller, which was formed as a result of the propeller-hull interaction, was obtained.

6. CONCLUSIONS

The present work is focused on the numerical prediction of KCS hull self- propulsion performance for working and without propeller conditions in model scale using RANS solution method. The validation study of KP505 propeller open water performance characteristics is firstly carried out. KP505 propeller open water CFD results showed an average error rate of 6.43% in K_T and 0.73% in K_Q based on test. When the hydrodynamic coefficients derived from the KCS hull self-propulsion performance analysis were compared with the test data, average error rates of 1.7% for K_T and 4.63% for K_Q were observed. The error rates of nominal and effective velocity coefficients between present CFD and test are 3,6 % and 0,12 % respectively. The other computed self-propulsion parameters, nominal and effective wake fields on propeller plane and pressure distribution on hull demonstrate a good agreement with measured results. The current numerical study reveals that the mesh element size should be determined by mesh sensitivity analysis, taking into account the effect of the mesh element size on the thrust and torque values. This approach provides the optimum mesh structure and closest numerical results to the test without requiring excessive solution time and high computer performance. The acceptable accuracy level of the current CFD simulations confirms the feasibility and reliability of the numerical method to predict the ship self-propulsion performance in order to quantify the hull-propeller interaction. Thus, it is approved that computational fluid dynamics methods can be used as a design tool for propeller and ship form development process instead of using towing tank that is much more expensive and time consuming way.

In this study, it has been observed that the CFD software provided a highly successful result in obtaining the pressure distribution occurring on the hull surface as a result of the propeller-hull interaction. The vibrations transmitted to the ship's structure due to the propeller-hull interaction can generate structural noise caused by pressure flactuation at the stern, potentially leading to significant issues. This structural noise arises as a consequence of fatigue induced by continuous vibrations, resulting in damage to various systems and structures within the vessel. Such damage adversely affects the operational performance of moving components and shortens their service

life. Furthermore, the resultant noise negatively impacts the comfort of both crew members and passengers, potentially leading to physical and psychological disturbances.

In future work, the propeller induced structural noise problems at the stern of the ship will be investigated. The finite element method will be used to analyze the hydrodynamic load distribution on the area above the propeller and the average structural noise level, as well as the effects of structural modifications aimed at reducing this noise.

ACKNOWLEDGEMENT

The author(s) declare(s) no conflict of interest.

REFERENCES

Carlton, J. S. (2006). *Marine propellers and propulsion (2nd ed.)*. Butterworth-Heinemann Ltd.

Carrica, P. M., Castro, A. M., & Stern, F. (2010). "Self-propulsion computations using a speed controller and a discretized propeller with dynamic overset grids." *Journal of Marine Science and Technology*, Vol.15, pp. 316–330. doi:10.1007/s00773-010-0098-6.

Carrica, P. M., Fu, H., & Stern, F. (2011). "Computations of self-propulsion free to sink and trim and of motions in head waves of the KRISO container ship (KCS) model." *Journal of Applied Ocean Research*, Vol.33, pp. 309–320. doi:10.1016/j.apor.2011.07.003.

Castro, A. M., Carrica, P. M., & Stern, F. (2011). "Full scale self-propulsion computations using discretized propeller for the KRISO container ship KCS." *Journal of Computers & Fluids*, Vol.51, pp. 35–47. doi:10.1016/j.compfluid.2011.07.003.

Feng, D., Ye, B., Zhang, Z., & Wang, X. (2020). "Numerical simulation of the ship resistance of KCS in different water depths for model-scale and full-scale." *Journal of Marine Science and Engineering*. doi:10.3390/jmse8100745.

Fujisava J., Ukon Y., Kume K., Takeshi H. (2000). "Local velocity field measurements around the KCS model (SRI M.S. No. 631) in the SRI 400M towing tank." *Report of Ship Performance Division*, Tokyo, Japan.

ITTC (International Towing Tank Conference), (2017). Uncertainty analysis in CFD verification and validation methodology and procedures.

ITTC Quality System Manual. (2014). Recommended procedures and guidelines: Open water test.

Kim J.. (2015). "Report of the results for KCS resistance & Self-Propulsion (Case 2-1, 2-5, and 2-7)." *A Workshop on CFD in Ship Hydrodynamics*. KRISO, Korea. https://www.t2015.nmri.go.jp.

Kinaci, O. K., Gokce, M. K., Alkan, A. D., & Kukner, A. (2018). "On self-propulsion assessment of marine vehicles." *Brodogradnja* , Vol.69, No.4, pp. 29-51, 2018. doi:10.21278/brod69403.

Seo, J. H., Seol, D. M., Lee, J. H., & Rhee, S. H. (2010). "Flexible CFD meshing strategy for prediction of ship resistance and propulsion performance." *International Journal of Naval Architecture and Ocean Engineering*, Vol. 2, pp. 139-145. doi:10.2478/IJNAOE-2013-0030.

Seok, W., Lee, S. B., & Rhee, S. H. (2019). "Computational simulation of turbulent flows around a marine propeller by solving the partially averaged Navier-Stokes equation." Proceedings of the Institution of Mechanical Engineers, Part C: *Journal of Mechanical Engineering Science*, Vol. 233, Issue 18, pp. 6357-6366. doi:10.1177/0954406219848021.

Shen, Z., Wan, D., & Carrica, P. M. (2015). "Dynamic overset grids in OpenFOAM with application to KCS self-propulsion and maneuvering." *Ocean Engineering*, Vol. 108, pp. 287–306. doi:10.1016/j.oceaneng.2015.07.035.

Tsukada Y., Hori T., Ukon Y., Kume K., Takeshi H. (2000). "Tokyo Surface pressure measurements on the KCS model (SRI M.S. No. 631) in the SRI 400M towing tank." *Report of Ship Performance Division*, Japan.

Wan, D., Wang, J., Liu, X., & Chen, G. (2016). "Numerical prediction of KCS self-propulsion in shallow water." *26th International Ocean and Polar Engineering Conference*, Rhodes, Greece, June 2016.

Zhang, Z. (2010). "Verification and validation for RANS simulation of KCS container ship without/with propeller". *Journal of Hydrodynamics*, Vol. 22, Issue 5, pp. 932-939.doi:10.1016/S1001-6058(10)60055-8.